Journal of Theoretical and Applied Information Technology
15th March 2024. Vol.102. No 5

ISSN: 1992-8645 www.jatit.org E-ISSN: 1817-3195

HEXAGONAL IMAGE COMPRESSION BASED ON WAVELET-GLOBAL THRESHOLDING

[1] I M. O. WIDYANTARA, [2]D. A. K. PRAMITA, [3]M. D. P. ASANA, [4]N. PRAMAITA, [5]I G. A. K. D. D. HARTAWAN, [6]J. K. MANI

[1,4,5]Udayana University, Department of Electrical Engineering, Denpasar, Bali

[2,3]Indonesian Institute of Business and Technology, Department of Informatic Engineering, Denpasar, Bali, Indonesia

[6]GITAM Deemed to be University, ITAM School of Technology, Bangalore, Karnataka, India

E-mail: [1]oka.widyantara@unud.ac.id, [2]pramita.wayu@instiki.ac.id, [3]dwiputraasana@instiki.ac.id., [4]n_pramaita@yahoo.com, [5]igakdiafari@unud.ac.id, [6]jmani@gitam.edu

ABSTRACT

This paper proposes a hexagonal grid image compression framework based on Wavelet thresholding. The target is to obtain optimal Rate-Distortion (RD) performance by implementing a threshold value prediction algorithm based on Global thresholding method. The compression scheme is built in two steps: resampling the hexagonal grid image and compressing it using the Wavelet-Global thresholding. The resampling process is carried out by alternating row and column suppression methods and an image interpolation method based on the Gabor Filter. In the Wavelet-Global thresholding, the coefficients of Gabor image are transformed into the Wavelet Coiflet, and the coefficients are thresholded globally using the Global thresholding. Furthermore, the quantization method and Arithmetic coding are applied to obtain a Hexagonal grid image compression scheme. The performance evaluation is performed on the Hard and Soft thresholding functions. Based on the threshold value generated by the Global thresholding, the Hard and Soft thresholding functions will limit the value of the Wavelet coefficients and impact the image's compression ratio and visual quality. The simulation results show that the best RD performance of the hexagonal grid image compression framework is obtained when applying a 1st order Coiflet filter with the Soft thresholding function

Keywords: *Hexagonal Grid Images, Gabor filter, Coiflet Wavelet filter, Global thresholding, Hard and Soft thresholding, Arithmetic coding, Rate-Distortion performance*

1. INTRODUCTION

Due to the effects of digital image processing and the internet, multimedia communication services must be available globally. This service requires high-quality digital images in various sizes and are generated in a short time. This situation led to an increased need for storage space on CDs and a demand for faster transmission of digital images over the internet. To avoid excessive use of space and to transmit images easily, compression methods are needed [1, 2].

Recent advances in image compression include transformation methods and entropy coding. Discrete Cosine Transform (DCT)/Discrete Wavelet Transform (DWT)-based transformation techniques and Huffman coding are still dominantly used to compress image data on JPEG [3] and JPEG 2000 [4, 5]. DCT and DWT-based image compression codecs have been used with Arithmetic coding to achieve higher compression, including DCT with Arithmetic Coding [6], significance-linked connected component analysis (SLCCA) [7, 8], Zerotree entropy coding [9, 10], and Set Partitions in a Tree Hierarchy (SPIHT) [11, 12]. The codec framework offers a high compression ratio while using a low number of bits per pixel (bpp). However, these codec formats are designed to process images in a rectangular grid.

Although the rectangular grid format is popular, there are numerous images whose pixels are arranged in a hexagonal pattern and are known as hexagonal grid images. In hexagonal grids, the information at the corners of the square image is omitted because it is rarely used to represent objects. This has the advantage of making the

spatial arrangement of the image more efficient and offering 13.4% fewer samples than rectangular grids. Hexagonal grids can also help reduce geometry distortion and aliasing effects in the image because the hexagonal shape is closer to a circle than a square [13–15]. In addition, the typical hexagonal grid in the structure of biological visual sensors, such as the compound eyes of insects [16], inspires computer vision researchers to pursue work in the field. Recently, hexagonal image processing has been applied to many areas, including edge detection [17], image registration [18, 19], ultrasound image processing [14], and machine vision and biomedical imaging [20].

In the context of image compression, the low percentage of pixels to be encoded and the better representation of various geometric shapes make image compression in hexagonal grid format has the potential to produce large compression ratios without compromising visual quality when reconstructed. Under these conditions, hexagonal grid image compression can achieve a balance between compression rate (smaller file size) and image quality that is acceptable to the user.

However, in the real world, we mainly use rectangular grids to make things easier to understand. Conventional imaging devices, including imaging sensors (CCD and CMOS) and displays, are primarily based on rectangular grids. Thus, to process the current hexagonal image, it is first necessary to re-sample from the original square grid, creating a hexagonal grid data. However, this resampling process can result in aliasing during the interpolation process and has an impact on decreasing the quality of the hexagonal grid image. A method using Gabor filters is proposed on a hexagonal grid to save on image reconstruction quality while providing additional computational advantages. Analysis was performed using the Windowing technique for better results [20, 21].

In the context of developing hexagonal grid image compression, researchers have proposed several frameworks focusing on (i) developing image resampling and interpolation methods and (ii) developing efficient image compression techniques. A Wavelet and DCT-based image compression framework for compressing Gabor-filtered hexagonal grid images has been proposed by Jeevan and Krishnakumar [22, 23]. This framework's hexagonal image compression ratio was not adaptive because it used a uniform threshold value for all Wavelet orders. Using a different threshold value for each wavelet sequence is a solution to get the best compression ratio, due to the varying intensities and spatial correlations in hexagonal images. Huaqing [24] has additionally suggested fractal-based hexagonal image reduction. This method uses Fractal Image Processing to generate improved fidelity with various compression ratios for all test images using spiral architecture for the hexagonal structure.

This research developed a Gabor-filtered hexagonal grid image compression scheme by applying the Wavelet thresholding method, where the threshold coefficients were generated using the Global Thresholding method. The implementation of Global Wavelet thresholding is needed to modify the Wavelet coefficient to zero to increase the compression ratio. Furthermore, a mechanism for comparing the performance of the Hard and Soft thresholding functions will be carried out to get the best hexagonal grid image compression performance by considering the RD parameters, namely the compression ratio and the visual quality of the reconstructed image.

The rest of the paper is organized as follows: Section 2 provides a detailed description of the proposed 2D DWT-based hexagonal grid image compression scheme, followed by results and its discussion in Section 3. Finally, the conclusions are described in section 4.

2. MATERIALS AND METHODS

This paper proposes a hexagonal grid image compression scheme based on 2D DWT. As shown in Figure 1, a hexagonal grid image is obtained by resampling the rectangular image and then interpolating Gabor to improve the image reconstruction quality [22]. The compression process begins by transforming the hexagonal image into coefficients using a 2D DWT filter bank. 2D DWT generates a sequence of Wavelet coefficients and separates them into low-frequency and high-frequency subbands. Furthermore, the Wavelet coefficients were quantized using a hard or soft threshold to create a stream symbol. Efficient encoding of stream symbols using Arithmetic-based entropy encoding produces a bit stream representing a compressed hexagonal image.

In some cases, the application of a hard threshold in quantizing the Wavelet coefficients causes blocky artefacts in hexagonal images. This is due to the prediction of wavelet coefficients based on fixed locations and variables. In addition, hexagonal images have their statistical distribution and differ in their characteristics depending on their subband.

Journal of Theoretical and Applied Information Technology
15th March 2024. Vol.102. No 5

ISSN: 1992-8645 www.jatit.org E-ISSN: 1817-3195

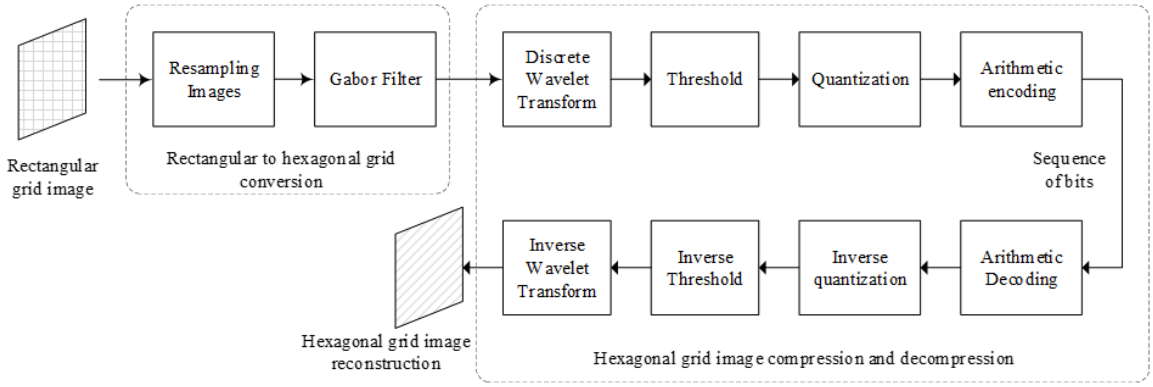

Figure 1: The proposed hexagonal grid image compression framework

To get a different threshold value at each Wavelet decomposition level, a level-dependent thresholding technique is proposed at this thresholding stage. A comparative analysis with the global thresholding technique will also be conducted to thoroughly assess the effectiveness of the suggested hexagonal image compression strategy.

2.1 Hexagonal Sampling System

The main limitation of using the hexagonal image structure is the lack of hardware to capture and display hexagonal-based images. For this reason, before to hexagonal-based image processing, a square image must be converted into a hexagonal image using the resampling method.

The resampling method used in this study is alternate suppressing rows and columns of a rectangular grid [25]. This approach suppresses any rectangular grid pixels that don't match up with those in the hexagonal part. It must be pressed to set this pixel's value to 0. When processing this sub-sampled image, the suppressed pixels aren't used in the computation. The sub-sampling procedure is based on the following rules:

$$y(i,j)=\begin{cases} x(2*i,2*j); & \text{if } i \text{ is even} \\ x(2*i,2*j+1); & \text{if } i \text{ is odd} \end{cases} \quad (1)$$

Where x(i,j) and y(i,j) are the pixel values in the row and column positions on the rectangular grid and the hexagonal grid, respectively.

As shown in Figure 2, during the acquisition of the image from the rectangular grid to the hexagonal grid, it was observed that there was a considerable decrease in image quality. So, selecting the appropriate interpolation technique is necessary before processing the image. Image reconstruction through interpolation is a routine task in image processing for all image transformations. The transformations include scaling, rotation, registration, and edge detection. On a hexagonal lattice, a method utilizing a Gabor filter is suggested to provide a higher quality of image reconstruction.

(a)

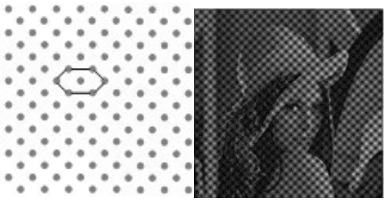

(b)

Figure 2: Image format and visuals, (a) Rectangular grid, (b) Hexagonal grid using Alternate Pixel Suppressal Method.

According to Manjunath and Ma [26], the typical definition of a two-dimensional Gabor function is utilized in this work. A two-dimensional Gabor function g(x,y) and its Fourier transform G(u,v) can be written as:

$$g(x,y)=\left(\frac{1}{2\pi\sigma_x\sigma_y}\right)\exp\left[-\frac{1}{2}\left(\frac{x^2}{\sigma_x^2}+\frac{y^2}{\sigma_y^2}\right)+2\pi jW_x\right] \quad (2)$$

In the frequency domain, it is expressed by:

$$G(u,v)=\exp\left\{-\frac{1}{2}\left[\frac{(u-W)^2}{\sigma_u^2}+\frac{v^2}{\sigma_v^2}\right]\right\} \quad (3)$$

where, $\sigma_u = 1/2\pi\sigma_x$ and $\sigma_v = 1/2\pi\sigma_y$. While σ_x and σ_y are the standard deviations of the elliptical Gaussian along the x and y axes.

A comprehensive but non-orthogonal basis set is formed by Gabor functions. An accurate localized frequency description can be obtained by expanding a signal on this basis. It is now time to think about a class of self-similar functions known as Gabor wavelets. Let g(x,y) be the mother Gabor wavelet; then, by appropriately dilating and rotating g(x,y) through the generating function, we can obtain the following self-similar filter dictionary:

$$g_{mn}(x,y) = a^{-m}G(x',y'), \quad a>1,\ m,n = \text{integer} \qquad (4)$$
$$x' = a^{-m}(x\cos\theta + y\sin\theta) \quad and \quad y' = a^{-m}(-x\sin\theta + y\cos\theta)$$

where $\theta = \frac{n\pi}{K}$ and K is the total number of orientations. The scale factor is meant to ensure that the energy does not depend on m.

2.2 2D DWT Decomposition

The signal is divided into energy bands sampled at various rates using the Discrete Wavelet Transform (DWT). This level is chosen to maintain the most signal information without reducing each sub-bands sample rate or resolution. Scaling and Wavelet functions, which are associated with low pass and high pass filters, respectively, are two sets of functions used by DWT. According to Nyquist's rule, half of the sample can be eliminated after each filtering stage because the signal's maximum frequency is π/2 rather than π. Therefore, the signal can be subsampled by 2 by eliminating every other sample. Figure 3 shows the two-dimensional (2-D) DWT's overall form.

At the decomposition level K, the order of the low and high-frequency coefficients can be expressed as follows:

$$X_L^{K+1}[n] = \sum_{l=0}^{N_L-1} g[l] \times X_L^K[2n-l] \qquad (5)$$

$$X_H^{K+1}[n] = \sum_{l=0}^{N_H-1} h[l] \times X_L^K[2n-1-l] \qquad (6)$$

where NH dan NL is the number of taps of each high pass filter (h) dan low pass filter (g).

Reconstruction of the 2D DWT decomposition bank filter is carried out at each level, where the input signal is first filtered along the row and then continued in the column direction. Mathematically, the 2-D DWT decomposition of the input signal Xi,j[n,m] is expressed as with n columns and m rows given by:

$$X_H^{K+1}[row,m] = \sum_{l=0}^{N_L-1} g[l] \times X_{LL}^K[row,2n-l]$$

$$X_H^{K+1}[row,m] = \sum_{l=0}^{N_H-1} h[l] \times X_{LL}^K[row,2m-1-l]$$

$$X_{LL}^{K+1}[n,col] = \sum_{l=0}^{N_L-1} g[l] \times X_L^K[2n-l,col]$$

$$X_{LH}^{K+1}[n,col] = \sum_{l=0}^{N_H-1} h[l] \times X_L^{K+1}[2n-1-l,col] \qquad (7)$$

$$X_{HL}^{K+1}[n,col] = \sum_{l=0}^{N_L-1} g[l] \times X_H^K[2n-l,col]$$

$$X_{HH}^{K+1}[n,col] = \sum_{l=0}^{N_H-1} h[l] \times X_H^K[2n-1-l,col]$$

where, $l = \{0, 1, \ldots, L-1\}$, $row = \{0, 1, \ldots, N/2^{K-1}\}$, $m = \{0, 1, \ldots, N/2^{K+1}-1\}$, $col = \{0, 1, \ldots, N/2^{K+1}-1\}$, $n = \{0, 1, \ldots, N/2^{K+1}-1\}$, and $X_{LL}^0[n,m] = X_{i,j}[n,m]$

2.3 Wavelet Filter

To perfectly synthesize the signal from the approximation and detail coefficients of DWT, this study used a lowpass and highpass filter from the mother Wavelet Coiflet [27]. Coiflet and Daubechies Wavelets are similar to some degree, but Coiflets are built with vanishing moments for Wavelet functions and scaling functions. Coiflets, as shown in Figure 4, are nearly symmetrical. The Wavelet function has N/3 vanishing moment and a scaling function, N/3 – 1, where N is the order of the Wavelet decomposition. The scaling function and the Wavelet function must be normalized by $1/\sqrt{2}$. The Coiflet scaling function has interpolation features, suggesting that this Wavelet enables an accurate approximation of the polynomial function at various resolutions.

2.4 Thresholding of Wavelet Coefficient

The Wavelet coefficients typically have values equal to or very close to zero in signals. The Wavelet coefficients can be changed by thresholding to produce additional zeros. Any coefficients below the threshold Y are set to zero in hard thresholding. It makes a lot of zeros and can have low bit rates when encoded using arithmetic encoding methods. To analyze the signal and eliminate Wavelet coefficients whose value is

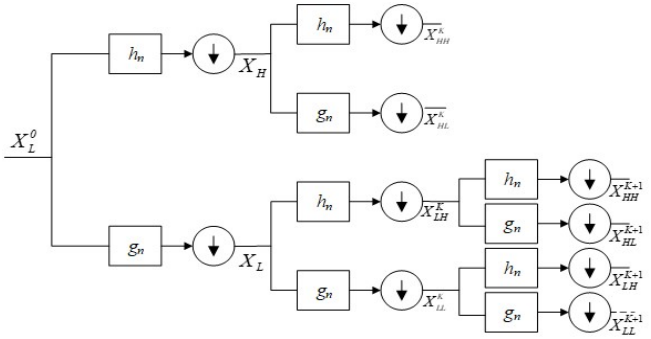

Figure 3: 2-D DWT Decomposition bank filter

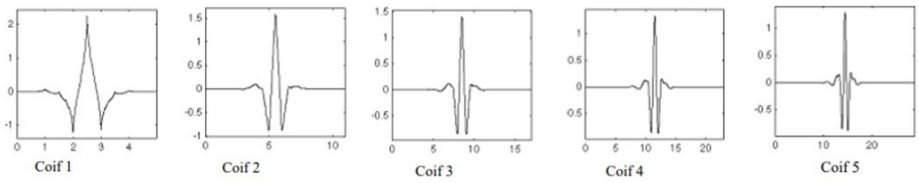

Figure 4: Coiflet Wavelet function

below the threshold value, Wavelet and thresholding are used. As a result, the compression rate increases as the number of zero Wavelet coefficients increases. Wavelet thresholding consists of two fundamental processes, namely.

2.4.1 *Thresholding Function Selection*

Thresholding functions commonly used in conjunction with DWT are Hard and Soft thresholding. The Wavelet coefficient for the hard threshold function at the decomposition level K is carried out as follows:

$$X_h^K(n,m)=\begin{cases} X^K(n,m), & |X^K(n,m)|>\lambda \\ 0, & others \end{cases} \quad (8)$$

As for the soft threshold function, the coefficients are stated as follows:

$$X_s^K(n,m)=\begin{cases} \mathrm{sgn}\left(X^K(n,m)\right)\left[|X^K(n,m)|-\lambda\right], & |X^K(n,m)|>\lambda \\ 0, & others \end{cases} \quad (9)$$

where is $X^K(n,m)$ the Wavelet coefficient, and λ is the threshold value. Elements with an absolute value lower than the threshold value will be set to zero, and the other coefficients will shrink. sgn(*) is a function:

$$\mathrm{sgn}(n)=\begin{cases} 1 & n>0 \\ -1 & n<0 \end{cases} \quad (10)$$

2.4.2 *Choosing the Optimal Threshold Value*

The threshold value determines the smoothness level of the Wavelet thresholding estimator. Choosing a threshold value that is too large will result in an estimate that is too smooth since the coefficients included in the reconstruction are too few. However, if a threshold value is chosen that is too small, it will result in an under-smooth estimation because too many coefficients are included in the reconstruction. Therefore, it is necessary to choose the optimal [28].

The Global thresholding technique selects one threshold parameter λ_j, to be used globally for all levels of decomposition j on the Wavelet coefficient $X^K(n,m)$. Donoho and Johnstone [29] presented the universal threshold by analyzing the normal Gaussian noise model. The formula for the universal threshold is given by:

$$\lambda=\sigma\sqrt{2\ln(N)} \quad (11)$$

Where σ is the mean-variance of the noise and N is the signal length. σ is calculated using the median estimation method with the formulation:

$$\sigma=\frac{Median\left(|X^K(n,m)|\right)}{0.6745} \quad (12)$$

Where $X^K(n,m)$ represents all Wavelet coefficients at the resolution level.

2.5 Quantization

DWT compression is achieved by quantization and entropy coding. Based on uniform quantization, the Wavelet coefficients are divided by a factor Q, and the results are rounded to the nearest number. In general, the quantitative index value is obtained by [30]:

$$I_q(n,m) = \frac{X^K(n,m) - X^K_{MIN}}{Q}$$
$$Q = \frac{(X^K_{MAX} - X^K_{MIN})}{L}$$
$$L = 2^N \quad (13)$$

where, X^K are the quantized Wavelet coefficients, X^K_{MAX}, X^K_{MIN}, are the maximum and minimum values of the subband Wavelet coefficients, respectively, and N is the number of bits used in quantization. Then, the quantization output value is:

$$X^K_q(m,n) = X^K_{Min} + I_q(m,n) * Q \quad (14)$$

where

$$I_q(n,m) = \begin{cases} I_q(n,m) - 1, if & I_q(n,m) = L \\ 0, & if \quad I_q(n,m) < 0 \end{cases} \quad (15)$$

2.6 Entropy coding by Arithmetic coding

As shown in Figure 5, Arithmetic Coding (AC) as a lossless compression mechanism assumes the input model is probabilistic and performs optimal compression with a given probability estimate [31]. The main idea in AC is to give each symbol a range or interval [0;1], where each range is divided into several subranges whose size is proportional to the probability. In this concept, AC replaces a row of input symbols with a floating number. The longer and more complex the encoded message, the more bits are needed for that purpose. The output of this arithmetic coding is a number that is less than one and greater than or equal to zero. To generate output numbers, each symbol to be encoded is assigned a set of probability values.

3. EXPERIMENTAL DETAILS

3.1 Experimental Setup

To assess the performance of the hexagonal grid image compression system, numerical experiments were carried out on several standard rectangular images measuring 512∗512 with 8 bits per pixel (bpp). In this paper, only the results related to the Lena and Baboon images are given as shown in Figure. 6.

Encoder:

a. Find the probability of each character in the text being encoded
Set value:
low_interval(*0*) = 0; *high_interval*(*0*) = 1; *range_interval*(*0*) = 1

b. *while not EOF*, read the *i-th* character do
low(*i*) = *low_interval*(*i* –1) + *range_interval*(*i* - 1) * *low_range_symbol*
high(*i*) = *low_interval*(*i* – 1) + *range_interval*(*i* - 1) * *high_range_symbol*
low_interval(*i*) = *low*(*i*)
high_interval(*i*) = *high*(*i*)
range_interval(*i*) = *high*(*i*) - *low*(*i*)

c. return

Decoder:

a. *output*(*0*) = the compression value

b. *while output*(i) != 0 do
output(*i*) = ((*output*(*I* - 1) - *low range symbol*))/((*high range symbol* - *low range symbol*))

Figure 5: Arithmetic Coding Algorithm

(a) *(b)*

Figure 6: Image Test, (a) Lena, (b) Baboon

The hexagonal grid image obtained by alternate suppressing of rectangular rows and columns is interpolated with a Gabor filter to improve image quality using equation (2). In this study, the location of the Gabor filter in 2D coordinates, g(x,y) is rounded from -1 to +1. Furthermore, the modulation coordinates (jW) for the spatial frequency are set to 11 and the corner frequency is set at 0°, 60°, and 120° to align with the hexagonal plane. Meanwhile, the values of x and y are each set to one, so the Fourier transforms σ_u and σ_v each have value.

The Gabor-filtered image is then transformed into a Wavelet using a mother Wavelet Coiflet. Table 1 shows the characteristics of the Coiflet filter used in this study. The Coiflet filter has a filter length of six times its order (6N) with a filter support width of 6N-1. The application of the Coiflet Wavelet filter is then analyzed to obtain the level of contribution of the transformation technique to the hexagonal image compression system. The implementation of the Coiflet Wavelet filter is up to a certain decomposition level (N). In

Table 1: Wavelet Coiflet filter characteristics

Wavelet Family	Coiflet
Abbreviation	Coif
Orde, N	1, 2, …, 5
Supporting Width	6N-1
Filter Length	6N
Filter Coefficient (transform)	
- LPF	-0.0156557, -0.0727326,0 .3848648, 0.8525720, 0.3378976, -0.0727326
- HPF	0.0727326, 0.3378976, -0.8525720, 0.3848648, 0.0727326, -0.0156557
Filter Coefficient (reconstruction)	
- LPF	0.0727326, 0.3378976, -0.8525720, 0.3848648, 0.0727326, -0.0156557
- HPF	-0.0156557, 0.0727326, 0.3848648, -0.8525720, 0.3378976, 0.0727326

this study, N was set 1, 2 and 3 to an enable analysis of the reconstructed image quality at different levels of decomposition. At each decomposition level, the Wavelet coefficients are obtained by hard and soft thresholds with the main limitation being the thresholding value generated by the Global Thresholding method. In this scheme, the Wavelet coefficients will be suppressed when they are above the global threshold coefficient at all levels of Wavelet decomposition. Furthermore, the Wavelet coefficients are compressed through the process of uniform quantization and arithmetic coding. In this study, the number of bits for the quantization process was set to 8 bits.

3.2 Evaluation Parameters

To get much better performance, the hexagonal grid image compression algorithm needs to achieve a trade-off between the bit rate and the reconstructed image quality that can be visualized in a Rate-Distortion (RD) graph. The bit rate is obtained by measuring the compression ratio, which is the percentage comparison of the Gabor-filtered image file size $X(i,j)$ with the image file size after Arithmetic Coding, $X'(n,m)$. The quality of the reconstructed image is measured by comparing the Gabor-filtered image $X(i,j)$ with the reconstructed image, $\hat{X}(i,j)$, which was obtained after the decompression process.

This study uses signal-to-noise ratio (PSNR) assessment [32] and rate-distortion analysis. PSNR is used to measure the quality of image reconstruction. The higher the PSNR value, the higher the similarity of the reconstructed image to the original image. PSNR is defined as follows:

$$PSNR = 20\log_{10}\left(\frac{Max_i}{\sqrt{MSE}}\right) = 10\log_{10}\left(\frac{255^2}{MSE}\right) \quad (16)$$

where MSE calculates the average of the square of the error defined as,

$$MSE = \sum_{i=0}^{M-1}\sum_{j=0}^{N-1}\left|X(i,j) - \hat{X}(i,j)\right| \quad (17)$$

where $X(i,j)$ is the Gabor-filtered Hexagonal grid image, $\hat{X}(i,j)$is the reconstructed image after the decompression process, and Max$i$ is the maximum possible pixel value of the image.

4. RESULTS AND DISCUSSIONS

The proposed hexagonal grid image compression method has been implemented and tested on standard test images. To obtain the contribution of Wavelet Thresholding and Arithmetic coding to the performance of hexagonal grid image compression, an evaluation of the comparison of the implementation of each Wavelet Coiflet with the same thresholding method was carried out. The experiment was carried out using an AMD Ryzen 5 3500U processor with Radeon Vega Mobile Gfx 2.10 GHz and a 64 bits operating system.

4.1 Image Filtered Gabor Analysis

Image pre-processing is performed to improve the visual quality of the hexagonal grid image using the Gabor filter. In line with equation (2), the performance of the Gabor filter on the visual quality of the image is shown in Table 2, where the best PSNR is obtained when the sigma value is set to 1. The Gabor-filtered image is free from false shadows and the texture features in the image are

Table 2: Gabor filter performance measurement

Hexagonal Image	PSNR (dB) at σ_x and σ_y		
	0,5	1	1,5
Lena	27,11	42,25	24,36
Baboon	27,11	35,17	24,61

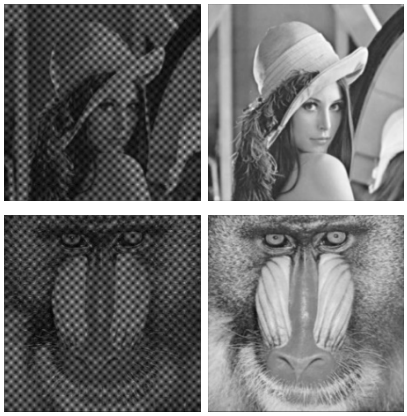

(a) (b)

Figure 7: Visual comparison of images, (a) Hexagonal grid image, (b) Gabor filtered Hexagonal Grid image

very clear compared to the original hexagonal image.

4.2 Hexagonal Grid Image Compression Performance

In this section, we first show that the threshold value (σ) generated by global thresholding changes in line with the increase in the Wavelet decomposition level. At the specified level, global thresholding calculates the median value of the Wavelet coefficients. The higher the order of the Wavelet, the lower the threshold value indicating the median value of the Wavelet coefficients on that order tends to decrease. As shown in Figures 8 and 9, based on the characteristics of the Coiflet filter in Table 2, the Wavelet coefficients in each order change so that the median value also changes.

Referring to equation (12), the threshold value generated by Global thresholding depends on the acquisition of the median value. Increasing the median value also increases the threshold value (σ), having an impact on increasing the values of the Wavelet coefficient which is set to zero. This condition causes the compression ratio of the hexagonal grid image to increase because many Wavelet coefficients do not need to be encoded arithmetic.

In the context of the compression concept, an increase in the compression ratio (CR) indicates that the hexagonal grid image compression framework can reduce the bit per pixel (bpp) allocation requirement across all orders and levels of Wavelet decomposition. As shown in Table 3, the implementation of the soft thresholding function on hexagonal grid image compression has a more optimal compression performance compared to the hard thresholding function of 0.33%, 0.51%, 0.52% for Lena images and 0.99%, 0.52%, 0.54% for Baboon images at the N1, N2 and N3 decomposition levels, respectively. This is possible because the hard thresholding function ignores Wavelet coefficients that are above the threshold value (λ). However, the soft thresholding function includes all values above the threshold value (λ) in the process of estimating the median value, assuming that any noise will affect all Wavelet coefficients.

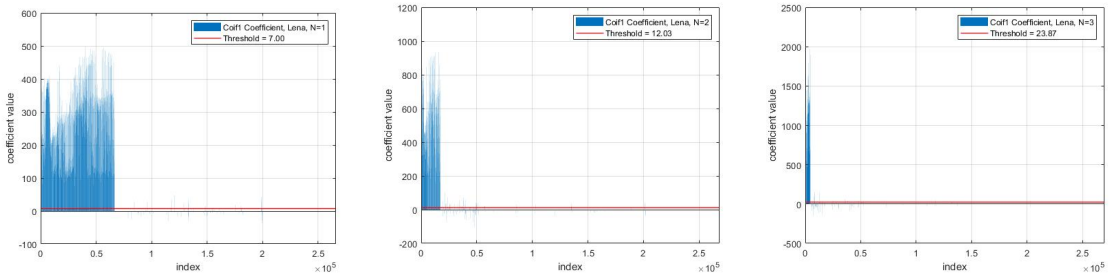

Figure 8: Comparison of Wavelet coefficients at decomposition level (N=1,2 and 3) with each Global Threshold value implemented in the hard thresholding function on Lena hexagonal image.

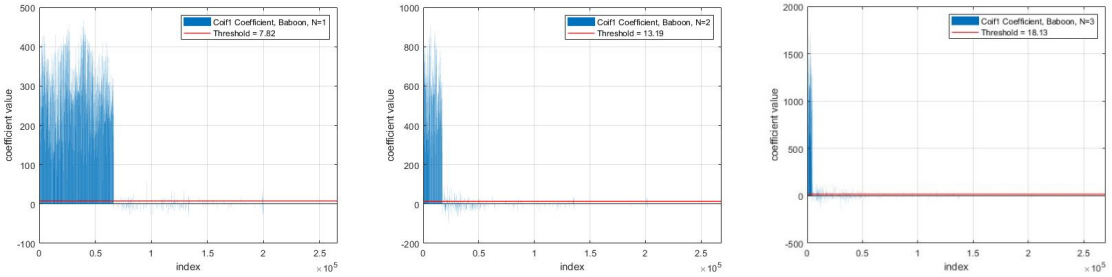

Figure 9: Comparison of Wavelet coefficients at decomposition level (N=1,2 and 3) with each Global Threshold value implemented in the hard thresholding function on Baboon hexagonal image.

Table 3: Compression ratio performance comparison

N	Performances	Lena Image					Baboon Image				
		Coif 1	Coif 2	Coif3	Coif4	Coif5	Coif 1	Coif 2	Coif3	Coif4	Coif5
1	Threshold Value	7,00	6,87	6,92	6,92	6,91	6,90	6,78	6,79	6,78	6,76
	CR of Hard Treshold (%)	33,84	34,59	33,92	33,15	32,44	30,34	32,64	32,75	32,38	31,84
	CR of Soft Threshold (%)	34,17	34,67	33,94	33,14	32,40	31,33	33,23	33,19	32,71	32,11
	Δ(%)	0,33	0,08	0,02	-0,02	-0,04	0,99	0,59	0,44	0,32	0,27
2	Threshold Values	12,03	11,29	10,75	10,73	10,79	12,67	12,76	12,70	12,63	12,58
	CR of Hard Treshold (%)	81,47	80,51	77,04	73,17	70,28	61,94	62,79	60,52	57,39	54,24
	CR of Soft Threshold (%)	85,62	83,40	79,40	75,50	72,71	66,37	66,50	63,77	60,02	57,30
	Δ(%)	0,51	0,51	0,51	0,51	0,51	0,52	0,51	0,51	0,51	0,51
3	Threshold Values	23,87	20,41	22,60	19,89	22,11	18,42	18,94	18,26	18,95	18,24
	CR of Hard Treshold (%)	170,20	148,12	144,30	124,18	119,78	97,44	94,50	84,78	78,49	70,19
	CR of Soft Threshold (%)	190,37	164,42	157,39	137,68	129,50	112,88	105,64	95,35	88,23	78,72
	Δ(%)	0,53	0,53	0,52	0,53	0,52	0,54	0,53	0,53	0,53	0,53

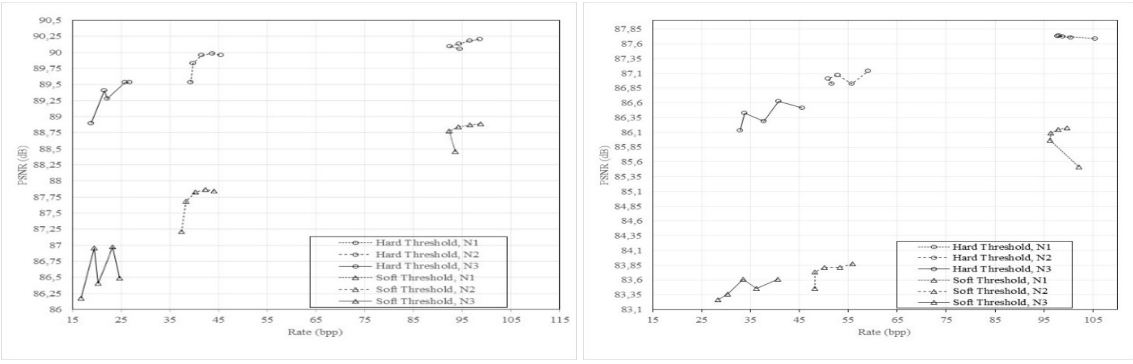

(a) *(b)*

Figure 10: Comparison of RD performance of hexagonal grid image compression on (a) Soft and (b) hard thresholding functions

As shown in Figures 10 and 11, the Rate-Distortion (RD) performance of hexagonal grid image compression by applying global thresholding to the hard and soft threshold functions is able to reduce the encoding rate while maintaining the visual quality of the image. This is indicated by the acquisition of PSNR values in all test images above 30 dB. Based on the conversion of PSNR values to

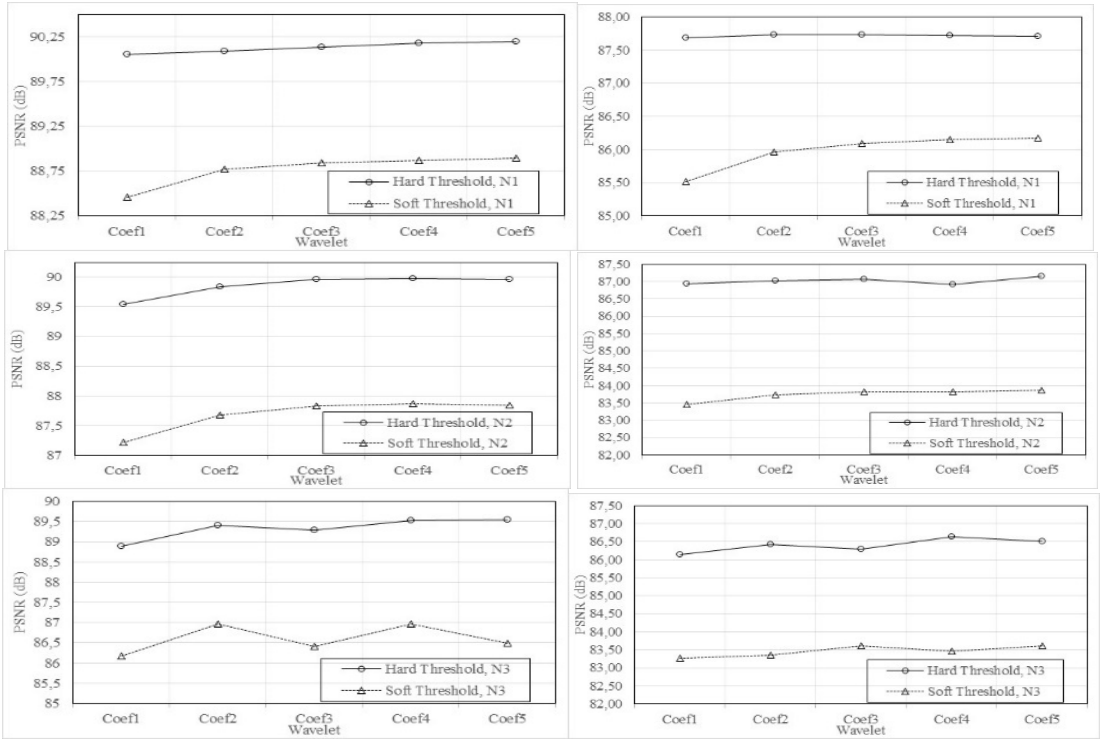

(a) (b)

Figure 11: PSNR performance of hexagonal grid image compression system using hard and soft thresholding functions on, (a) Lena image, and (b) Baboon image

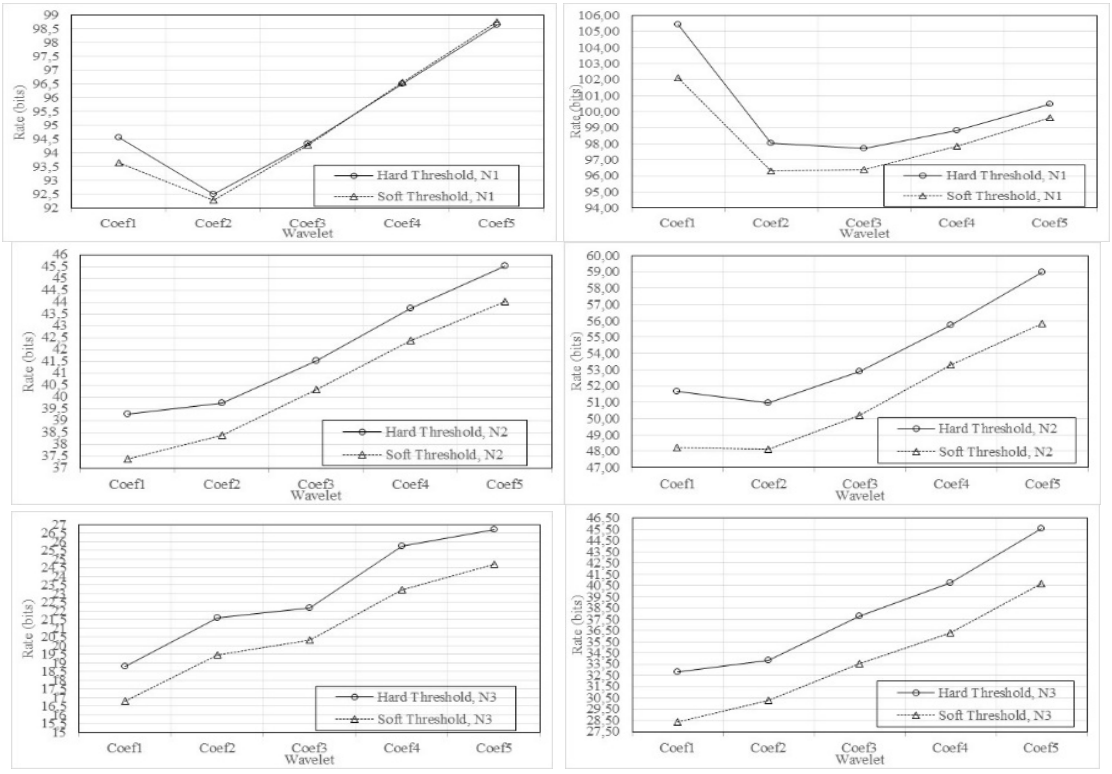

(a) (b)

Figure 12: Bit rate performance for a hexagonal grid image compression framework using hard and soft thresholding functions on, (a) Lena images, and (b) Baboon images

the Mean Opinion Score (MOS) table [33], the obtained PSNR compression of the hexagonal grid image is in the excellent category.

The bit rate performance analysis, as shown in Figure 12, shows that the application of the first-order Coiflet Wavelet filter can optimally contribute to reducing the bitrate compression of the hexagonal grid image to 18.80 bpp and 16.81 bpp at decomposition level 3, respectively, for the hard and hard functions soft thresholding. The application of the soft thresholding function by the largest compression ratio of the hexagonal grid image compression system contributes to this result.

5. CONCLUSION

This paper proposes a hexagonal grid image compression framework using threshold-predicting Wavelet and Arithmetic coding. In this framework, the Gabor filter was implemented at the pre-processing stage of the hexagonal grid image, and the Coiflet Wavelet filter, Global thresholding with hard and soft threshold functions, quantization, and Arithmetic coding at the image compression stage. The implementation of Global Wavelet thresholding is needed to modify the Coiflet Wavelet coefficient to zero to increase the compression ratio. A mechanism for comparing the performance of the Hard and Soft thresholding functions is carried out to get the best hexagonal grid image compression performance.

The experimental results show that the Gabor filter can improve the visual quality of the hexagonal grid image after the resampling process. Evaluation of RD performance also indicates that the hexagonal grid image compression framework can produce an optimal compression ratio while maintaining the image's visual quality at an excellent level on the MOS standard.

ACKNOWLEDGEMENTS

The highest gratitude is conveyed to the Institute for Research and Community Service and the Faculty of Engineering, Udayana University providing funds for this research.

REFERENCES

[1] Akhtarkavan, E., and Salleh, M. F. M. "Multiple Descriptions Coinciding Lattice Vector Quantizer for Wavelet Image Coding." *IEEE Transactions on Image Processing*, Vol. 21, No. 2, (2012), 653–661. https://doi.org/10.1109/TIP.2011.2164419

[2] Zhou, Y., Wang, C., and Zhou, X. "DCT-Based Color Image Compression Algorithm Using an Efficient Lossless Encoder." In *2018 14th IEEE International Conference on Signal Processing (ICSP)* (pp. 450–454). IEEE. https://doi.org/10.1109/ICSP.2018.8652455

[3] Wallace, G. K. "The JPEG still picture compression standard." *IEEE Transactions on Consumer Electronics*, Vol. 38, No. 1, (1992), xviii–xxxiv. https://doi.org/10.1109/30.125072

[4] Al-Shaykh, O. K., Moccagatta, I., and Homer Chen. "JPEG-2000: a new still image compression standard." In *Conference Record of Thirty-Second Asilomar Conference on Signals, Systems and Computers (Cat. No.98CH36284)* (pp. 99–103). IEEE. https://doi.org/10.1109/ACSSC.1998.750835

[5] Barda, J. F. "JPEG 2000, the next millennium compression standard for still images." In *Proceedings IEEE International Conference on Multimedia Computing and Systems* (pp. 1126–1127). IEEE Comput. Soc. https://doi.org/10.1109/MMCS.1999.778678

[6] Chikouche, D., Benzid, R., and Bentoumi, M. "Application of the DCT and Arithmetic Coding to Medical Image Compression." In *2008 3rd International Conference on Information and Communication Technologies: From Theory to Applications* (pp. 1–5). IEEE. https://doi.org/10.1109/ICTTA.2008.4530107

[7] Jiang, X., Song, B., and Zhuang, X. "An Enhanced Wavelet Image Codec: SLCCA PLUS." In *2018 International Conference on Audio, Language and Image Processing (ICALIP)* (pp. 163–167). IEEE. https://doi.org/10.1109/ICALIP.2018.8455373

[8] Vass, J., and Zhuang, X. "Enhanced significance-linked connected component analysis for high performance error resilient Wavelet image coding." In *Proceedings 15th International Conference on Pattern Recognition. ICPR-2000* (pp. 71–74). IEEE Comput. Soc. https://doi.org/10.1109/ICPR.2000.903488

[9] Shapiro, J. M. "Embedded image coding using Zerotrees of Wavelet coefficients." *IEEE Transactions on Signal Processing*, Vol. 41, No. 12, (1993), 3445–3462. https://doi.org/10.1109/78.258085

[10] Boujelbene, R., Boubchir, L., and ben Jemaa, Y. "Enhanced embedded zero tree Wavelet algorithm for lossy image coding." *IET Image*

Processing, Vol. 13, No. 8, (2019), 1364–1374. https://doi.org/10.1049/iet-ipr.2018.6052

[11] Tunga P., P., and Singh, V. "Compression of MRI brain images based on automatic extraction of tumor region." *International Journal of Electrical and Computer Engineering (IJECE)*, Vol. 11, No. 5, (2021), 3964. https://doi.org/10.11591/ijece.v11i5.pp3964-3976

[12] Imane, H., Mohammed, B., and Ahmed, B. "Hybrid medical image compression method using quincunx Wavelet and geometric active contour." *Bulletin of Electrical Engineering and Informatics*, Vol. 9, No. 1, (2020), 146–159. https://doi.org/10.11591/eei.v9i1.1675

[13] Qingtang Jiang. "FIR Filter Banks for Hexagonal Data Processing." *IEEE Transactions on Image Processing*, Vol. 17, No. 9, (2008), 1512–1521. https://doi.org/10.1109/TIP.2008.2001401

[14] Contreras-Ortiz, S. H., and Fox, M. D. "Hexagonal filters for ultrasound images." *Journal of Electronic Imaging*, Vol. 23, No. 4, (2014), 043022. https://doi.org/10.1117/1.JEI.23.4.043022

[15] Firouzi, M., Fadaei, S., and Rashno, A. "A New Framework for Canny Edge Detector in Hexagonal Lattice." *International Journal of Engineering*, Vol. 35, No. 8, (2022), 1588–1593. https://doi.org/10.5829/IJE.2022.35.08B.15

[16] Vanhoutte, K. J. A., Michielsen, K. F. L., and Stavenga, D. G. "Analyzing the reflections from single ommatidia in the butterfly compound eye with Voronoi diagrams." *Journal of Neuroscience Methods*, Vol. 131, No. 1–2, (2003), 195–203. https://doi.org/10.1016/j.jneumeth.2003.08.011

[17] Middleton, L., and Sivaswamy, J. "Edge detection in a hexagonal-image processing framework." *Image and Vision Computing*, Vol. 19, No. 14, (2001), 1071–1081. https://doi.org/10.1016/S0262-8856(01)00067-1

[18] Shima, T., Sugimoto, S., and Okutomi, M. "Comparison of image alignment on hexagonal and square lattices." In *2010 IEEE International Conference on Image Processing* (pp. 141–144). IEEE. https://doi.org/10.1109/ICIP.2010.5654351

[19] Argyriou, V. "Sub-Hexagonal Phase Correlation for Motion Estimation." *IEEE Transactions on Image Processing*, Vol. 20, No. 1, (2011), 110–120. https://doi.org/10.1109/TIP.2010.2057438

[20] Veni, S., and Narayanankutty, K. A. "Vision-based hexagonal image processing using Hex-Gabor." *Signal, Image and Video Processing*, Vol. 8, No. 2, (2014), 317–326. https://doi.org/10.1007/s11760-012-0293-5

[21] Veni, S., and Narayanankutty, K. A. "Image enhancement of medical images using Gabor filter bank on hexagonal sampled grids." *World Academy of Science, Engineering and Technology*, Vol. 65, (2010), 816–821.

[22] Jeevan, K. M., and Krishnakumar, S. "Compression of images represented in hexagonal lattice using Wavelet and Gabor filter." In *2014 International Conference on Contemporary Computing and Informatics (IC3I)* (pp. 609–613). IEEE. https://doi.org/10.1109/IC3I.2014.7019622

[23] Mani, J. K., A, R. R., and Krishnakumar, S. "Performance Comparison of DCT Based Image Compression on Hexagonal and Rectangular Sampling Grid." *Journal of Image and Graphics*, Vol. 1, No. 3, (2013), 153–156. https://doi.org/10.12720/joig.1.3.153-156

[24] Huaqing Wang, Xiangjian He, Qiang Wu, and Hintz, T. "A New Approach for Fractal Image Compression on a Virtual Hexagonal Structure." In *18th International Conference on Pattern Recognition (ICPR'06)* (pp. 909–912). IEEE. https://doi.org/10.1109/ICPR.2006.1

[25] Senthilnayaki, M., Veni, S., and Kutty, K. A. "Hexagonal Pixel Grid Modeling for Edge Detection and Design of Cellular Architecture for Binary Image Skeletonization." In *2006 Annual IEEE India Conference* (pp. 1–6). IEEE. https://doi.org/10.1109/INDCON.2006.302802

[26] Manjunath, B. S., and Ma, W. Y. "Texture features for browsing and retrieval of image data." *IEEE Transactions on Pattern Analysis and Machine Intelligence*, Vol. 18, No. 8, (1996), 837–842. https://doi.org/10.1109/34.531803

[27] Sridhar, S., Rajesh Kumar, P., and Ramanaiah, K. V. " Wavelet Transform Techniques for Image Compression – An Evaluation." *International Journal of Image, Graphics and Signal Processing*, Vol. 6, No. 2, (2014), 54–67. https://doi.org/10.5815/ijigsp.2014.02.07

[28] Hall, P., and Patil, P. "On the Choice of Smoothing Parameter, Threshold and Truncation in Nonparametric Regression by Non-Linear Wavelet Methods." *Journal of the*

Royal Statistical Society: Series B (Methodological), Vol. 58, No. 2, (1996), 361–377. https://doi.org/10.1111/j.2517-6161.1996.tb02087.x

[29] Donoho, D. L., and Johnstone, I. M. "Ideal spatial adaptation by wavelet shrinkage." *Biometrika*, Vol. 81, No. 3, (1994), 425–455. https://doi.org/10.1093/biomet/81.3.425

[30] Tan, L., and Jiang, J. "Signal Sampling and Quantization." In *Digital Signal Processing* (pp. 13–58). Elsevier. https://doi.org/10.1016/B978-0-12-815071-9.00002-6

[31] Masmoudi, A., Puech, W., and Masmoudi, A. "An improved lossless image compression based arithmetic coding using mixture of non-parametric distributions." *Multimedia Tools and Applications*, Vol. 74, No. 23, (2015), 10605–10619. https://doi.org/10.1007/s11042-014-2195-8

[32] Hore, A., and Ziou, D. "Image Quality Metrics: PSNR vs. SSIM." In *2010 20th International Conference on Pattern Recognition* (pp. 2366–2369). IEEE. https://doi.org/10.1109/ICPR.2010.579

[33] Klaue, J., Rathke, B., and Wolisz, A. "EvalVid – A Framework for Video Transmission and Quality Evaluation." In *13th International Conference on Modelling Techniques and Tools for Computer Performance* (pp. 255–272). https://doi.org/10.1007/978-3-540-45232-4_16